Persistent Positive North Atlantic Oscillation Mode Dominated the Medieval Climate Anomaly

Valérie Trouet, *et al.*

Science **324**, 78 (2009);
DOI: 10.1126/science.1166349

Science (print ISSN 0036-8075; online ISSN 1095-9203) is published weekly, except the last week in December, by the American Association for the Advancement of Science, 1200 New York Avenue NW, Washington, DC 20005.

Persistent Positive North Atlantic Oscillation Mode Dominated the Medieval Climate Anomaly

Valérie Trouet,[1]* Jan Esper,[1,2] Nicholas E. Graham,[3,4] Andy Baker,[5] James D. Scourse,[6] David C. Frank[1]

The Medieval Climate Anomaly (MCA) was the most recent pre-industrial era warm interval of European climate, yet its driving mechanisms remain uncertain. We present here a 947-year-long multidecadal North Atlantic Oscillation (NAO) reconstruction and find a persistent positive NAO during the MCA. Supplementary reconstructions based on climate model results and proxy data indicate a clear shift to weaker NAO conditions into the Little Ice Age (LIA). Globally distributed proxy data suggest that this NAO shift is one aspect of a global MCA-LIA climate transition that probably was coupled to prevailing La Niña–like conditions amplified by an intensified Atlantic meridional overturning circulation during the MCA.

The North Atlantic Oscillation (NAO)—the main synoptic mode of atmospheric circulation and climate variability in the North Atlantic/European sector—has a substantial influence on marine and terrestrial ecosystems and regional socio-economic activity (*1*). Because the instrumental record of the NAO is relatively short (*2*), there is a need for information on its long-term variability to better understand climate variability in the more distant past and to assess NAO predictability. An array of multiproxy approaches has been applied to extend the NAO record back in time (*3*); however, these only extend to 1400 A.D. and do not span the MCA (*4*), a period (~800–1300) marked by a wide range of changes in climate globally, including apparent relative warmth over the North Atlantic/European sector and much of the extra-tropical Northern Hemisphere (*5*). The MCA is the most recent natural counterpart to modern warmth and can therefore be used to test characteristic patterns of natural versus anthropogenic forcing.

A recent tree-ring–based drought reconstruction for Morocco (1049–2002) (*6*) and a millennial-length speleothem-based precipitation proxy for Scotland (900–1993) (*7*), strategically sited and sensitive to atmospheric variations in the southern and northern nodes of the NAO dipole, provide us with a basis for extending the instrumental winter NAO index (*8*) back to the MCA (Fig. 1) (*9*). Over the 20th century, correlations between instrumental (*10*) Scotland and Morocco December-to-March precipitation and the NAO (*2*) are 0.75 and –0.64, respectively. The Morocco and Scotland reconstructions contain substantial multidecadal variability that is characterized by antiphase oscillatory behavior over the last millennium. The Scotland speleothem record is remarkably similar to Lamb's reconstruction (*4*) of England-Wales September-to-June precipitation (fig. S1), with a sharp 10% decrease in inferred precipitation between the late 13th to mid-14th centuries, a continued decline through the mid-16th to late 18th centuries, and an increasing trend toward present. Contrasting moisture conditions between the Morocco and the Scotland proxy series were particularly strong between 1050 and 1400, during the 18th century, and since the 1940s. A strong inverse relation is also found when comparing observational precipitation records (*10*) for Scotland and Morocco (Pearson correlation coefficient $r = -0.49$, $P < 0.01$ for 1940–2001).

We identified periods of opposing values in the Scotland and Morocco proxies as extremes in the residual series (NAO_{ms}), calculated as the difference between the 30-year smoothed and normalized Scotland and Morocco records (*9*). We used NAO_{ms} as a proxy for decadal-scale winter NAO variability back to 1050. NAO_{ms} reveals multidecadal variability over the 20th century similar to that seen in smoothed instrumental NAO time series (*2*, *11*), including a high-index phase from the turn of the 20th century until the 1930s, a minimum in the 1960s, and an increase since the 1970s (fig. S2). In the 19th century, coherence between the individual instrumental NAO series decreases, probably representing increasing uncertainty back in time, which is typical for both proxy and instrumental data (*12*). Interdecadal fluctuations in NAO_{ms} correspond well with the variability reflected by other NAO reconstructions (*3*, *13*, *14*) (Fig. 2 and table S1). NAO_{ms} is 350 years longer than Cook's reconstruction (*3*) and covers the latter part of the MCA (1050–1400), a period over which NAO_{ms} values were persistently positive compared with the 1500–1983 reference period.

Multidecadal fluctuations in a winter temperature-sensitive $\delta^{18}O$ record from a speleothem in the European Alps (*15*) match the fluctuations in NAO_{ms} over the full period of the record (fig. S1), which is in correspondence with the known relation between the NAO, variability in the strength of winter westerlies across Europe, and winter temperatures across northern and central Europe (*11*). In the low-frequency domain, these winter changes are similar to reconstructed European annual and summer temperatures. In addition, reconstructed European winter sea-level pressure (SLP), temperature (*16*), and precipitation (*17*) patterns, composited for positive and negative NAO_{ms} phases, correspond well with longer-term NAO signatures since 1659 (Fig. 3A). The increased pressure difference between the Azores High (+3 hPa) and the Icelandic Low (–5 hPa) during positive NAO phases results in enhanced zonal flow, with stronger westerlies transporting warm air to the

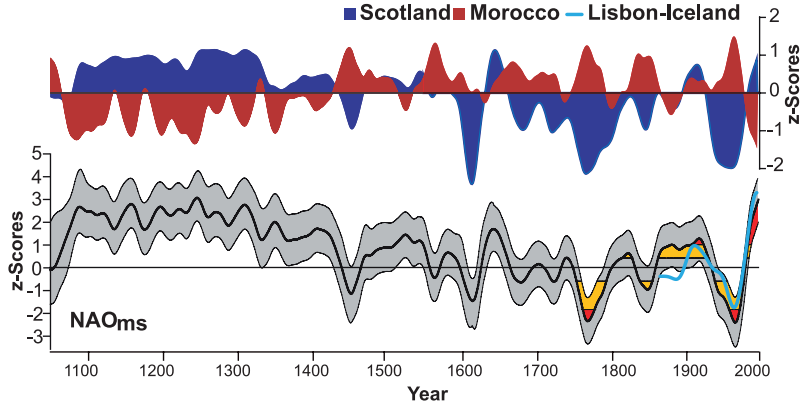

Fig. 1. Proxy-derived long-term NAO reconstruction. (**Top**) Reconstructed winter precipitation for Scotland and February-to-June Palmer Drought Severity Index (*29*) for Morocco. Records were normalized over the common period (1049–1995) and smoothed with the use of a 30-year cubic spline. (**Bottom**) Winter NAO reconstruction NAO_{ms} (black curve) is the difference of the Scotland and Morocco records. The gray area is the estimated uncertainty; yellow and red areas are the 10 and 33% highest and lowest values since 1700. The blue line represents the 30-year smoothed Lisbon-Iceland instrumental NAO index series (*11*).

[1]Swiss Federal Institute for Forest, Snow, and Landscape Research (WSL), Zürcherstrasse 111, 8903 Birmensdorf, Switzerland. [2]Oeschger Centre for Climate Change Research, Erlachstrasse 9a, 3012 Bern, Switzerland. [3]Hydrologic Research Center, 12780 High Bluff Drive, Suite 250, San Diego, CA 92130–2069, USA. [4]Scripps Institution of Oceanography, 9500 Gilman Drive, La Jolla, CA 92093–0225, USA. [5]School of Geography, Earth and Environmental Sciences, University of Birmingham, Birmingham, B15 2TT, UK. [6]School of Ocean Sciences, University of Wales Bangor, Menai Bridge, Anglesey, LL59 5AB, UK.

*To whom correspondence should be addressed. E-mail: trouet@wsl.ch

European continent. The axis of maximum moisture transport and the preferred storm track extend further to the north and east during positive NAO phases when the Azores High is strengthened, resulting in wetter winters over northwestern Europe (50-to-200–mm positive anomalies per season) and decreased precipitation over southern Europe and northwestern Africa (50-to-100–mm negative anomalies per season).

We used a proxy-model analog method [proxy surrogate reconstruction (PSR) (*18*)] to develop a more complete synoptic understanding of the changes associated with the reconstructed NAO dynamics (*9*). In PSR, data from coupled ocean-atmosphere general circulation model (CGCM) simulations are reordered to maximize temporal agreement between multiple proxy records and commensurate data drawn from the model output. The reordered model data set can be used to more fully characterize climate patterns implied by sparse and diverse proxy data. Specifically, in this study, December-to-March precipitation and temperature CGCM data are conditioned on the proxy precipitation records from Scotland (*7*) and Morocco (*6*) and a winter temperature record from the Alps (*15*).

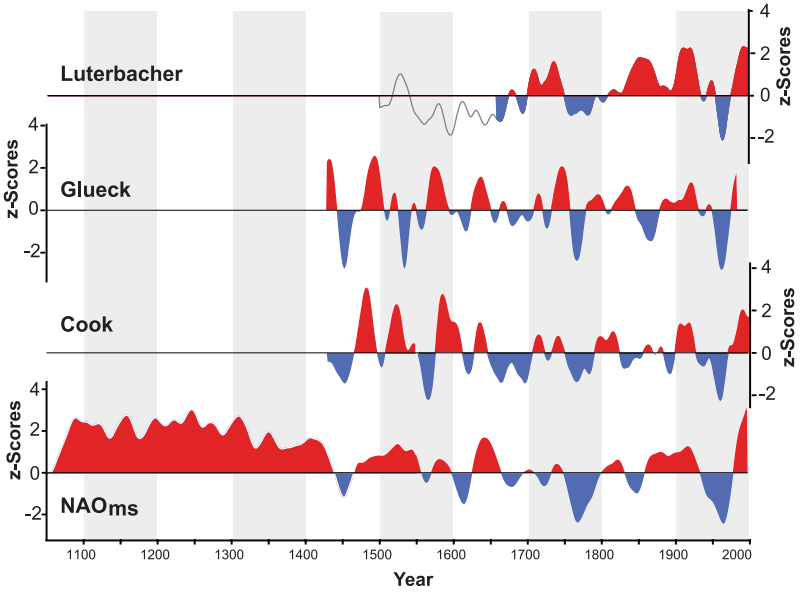

Fig. 2. Proxy-based NAO reconstructions. NAO_{ms} compared with reconstructions by Cook *et al.* (*3*), Glueck and Stockton (*13*), and Luterbacher *et al.* (*14*). All series were smoothed with the use of a 30-year spline and normalized over the 1500-to-1983 common period. The blank period in the Luterbacher reconstruction represents the period before 1659, for which only seasonal values were available.

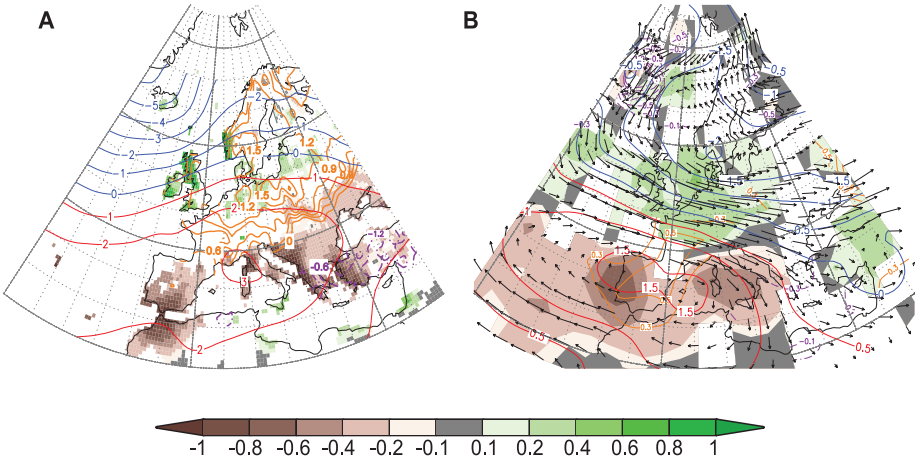

Fig. 3. Empirical and model-derived NAO patterns. Proxy and instrumental (*16*, *17*) (1659–1995) (**A**) and PSR (*18*) reconstructed [with Max Planck Institute model data (*19*)] (**B**) fields of December-to-February SLP, temperature, and precipitation were composited for positive and negative NAO phases. NAO phases were determined in (A) as the 10% most positive versus the 10% most negative NAO_{ms} winters (1659–1995) (Fig. 1) and in (B) as average values for the period 1049–1298 minus those for 1448–1923. Composite difference maps are shown for SLP (red and blue contours, in meters), temperature (orange and dashed purple contours, in degrees Celsius), and precipitation (shaded areas, in millimeters). Shaded areas and contours reflect significant ($P < 0.1$) differences, calculated with a *t* test.

Figure 3B shows composite differences between the MCA and the Little Ice Age (LIA) (averages for 1049–1298 minus those for 1448–1923) in December-to-March SLP, precipitation, and near-surface temperature from the PSR reconstruction, based on a 240-year simulation with the Max Planck Institute coupled ECHAM4-OPYC model (*19*). At the three proxy-model comparison points, the agreement between the input proxy- and model-derived series is close, with correlations of 0.94, 0.94, and 0.92 for Morocco precipitation, Alps temperature, and Scotland precipitation, respectively. Results show an SLP dipole with centers over southern Scandinavia (–2 hPa) and across Iberia (+1.5 hPa) and increased westerlies across western Europe. Considering uncertainties (supporting online text), a plausible range for the magnitude of the PSR-reconstructed MCA-LIA NAO difference is 1.5 to 6.0 hPa. For comparison, the late 20th century upward swing in the NAO was ~7.5 hPa. Increased precipitation over the northeast Atlantic extends across the British Isles and into northwestern Europe (20-to-40–mm positive anomalies per season), and decreased precipitation extends across northwestern Africa, Iberia, and south-central Europe (20-to-50–mm negative anomalies). MCA-to-LIA winter temperature differences of 0.3° to 0.5°C cover most of western Europe with the largest amplitude over Iberia and southern France. The reconstruction suggests an MCA-LIA decrease of westerlies on the order of 0.8 to 1.2 ms^{-1}, a decline of 10 to 20%. Similar patterns and magnitudes found using National Center for Atmospheric Research Community Climate System Model data (fig. S3C) (*20*) suggest that results do not depend on the particular model used in the study.

The persistently strong winter MCA NAO and its weakening during the LIA raise questions about the mechanism responsible for producing such a temporally pervasive atmospheric state over the North Atlantic, as well as MCA-LIA climate anomalies elsewhere (Fig. 4). The widespread signature of this climatic shift implies that changes in tropical sea surface temperatures (SSTs) were involved. A possible explanation is that heating of the western equatorial Pacific (*21*, *22*) and of the tropical Indian Ocean (*23*) induced decreased eastern and central tropical Pacific SSTs resulting in an initial strengthening of the NAO through tropospheric dynamics (*18*, *24*). This modeled La Niña–like state during the MCA is supported by marine proxy records (Fig. 4C and table S2) that show warm SST anomalies in the western tropical Pacific during the MCA (*25*) and cool SSTs in the central and eastern tropical Pacific (*26*).

Stronger westerlies associated with a prolonged positive NAO phase may have enhanced the Atlantic meridional overturning circulation

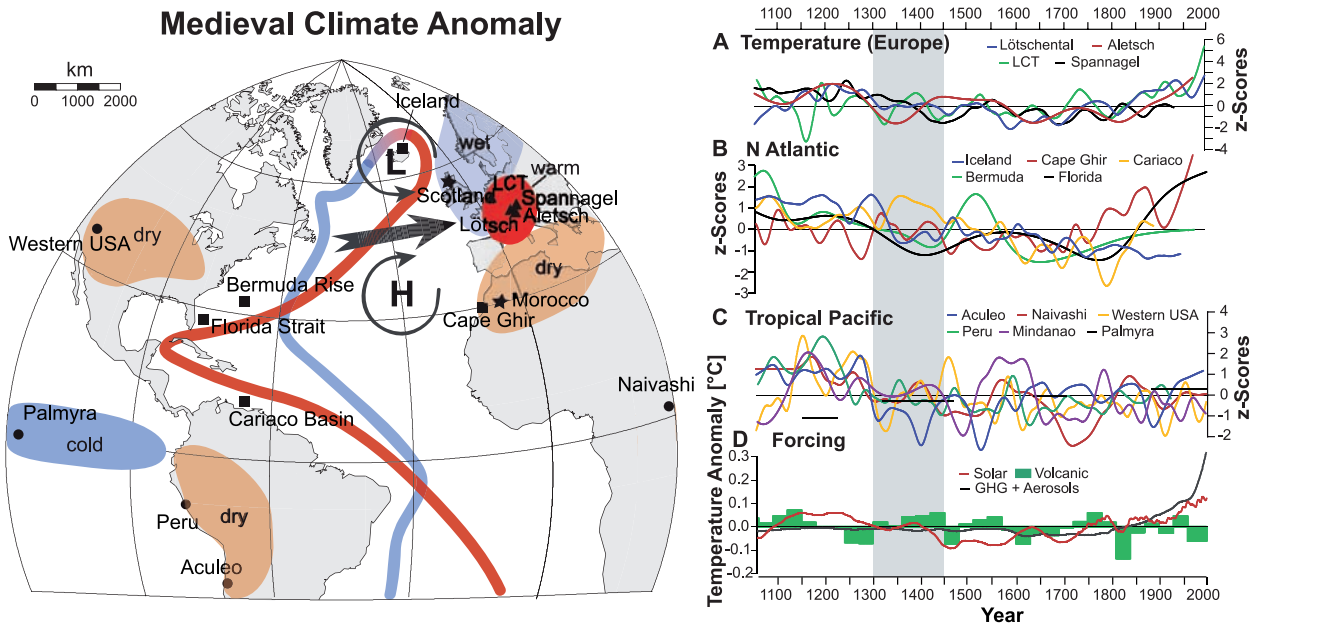

Fig. 4. Large-scale Medieval Climate Anomaly pattern. Geographical location and time series (1050–2000) of proxy records of European temperatures [(**A**), black triangles in the map at left], North Atlantic conditions [(**B**), black squares], tropical Pacific conditions [(**C**), black circles], and external forcings (**D**). Records in (A) to (C) were smoothed with a 60-year spline and normalized over the full period. References for all records are provided in table S1. The radiative forcing time series is derived from (*30*) with the volcanism time series consisting of 30-year averages. The 1300-to-1450 MCA-LIA transition period is highlighted in gray. The map indicates inferred climatic conditions and an intensified AMOC during the MCA, as derived from the proxy records. L, Icelandic Low; H, Azores High.

(AMOC) (*27*), which, in turn, generated cross-equatorial salinity and SST anomalies in the tropical Atlantic and a related northward migration of the intertropical convergence zone (*28*). An enhanced AMOC may have accommodated a constructive feedback mechanism, proxy evidence for which is provided by North Atlantic records (Fig. 4B and table S2), that reinforced the La Niña–like conditions in the tropical Pacific (*22*).

Independent of temperature indicators, the persistent positive NAO phase reconstructed for the MCA now provides a dynamical explanation of winter warmth over Europe during Medieval times (Fig. 4A). Whereas non-stationarity is a general challenge for proxy-based reconstructions, the records used here originate from locations that were shown to lie consistently within the influence of the northern and southern nodes of the NAO dipole (*3*). To help overcome the reduced degrees of freedom in the low-frequency domain that generally limit possibilities for calibration, our proxy-based reconstruction was additionally supported by physically plausible PSR-based synoptic fields. The persistent positive phase reconstructed for the MCA appears to be associated with prevailing La Niña–like conditions possibly initiated by enhanced solar irradiance and/or reduced volcanic activity (*21*) (Fig. 4D) and amplified and prolonged by enhanced AMOC. The relaxation from this particular ocean-atmosphere state into the LIA appears to be globally contemporaneous and suggests a notable and persistent reorganization of large-scale oceanic and atmospheric circulation patterns.

References and Notes

1. J. W. Hurrell, Y. Kushnir, G. Ottersen, M. Visbeck, in *Geophysical Monograph Series 134*, (American Geophysical Union, Washington, DC, 2003), pp. 1–35.
2. P. D. Jones, T. Jonsson, D. Wheeler, *Int. J. Climatol.* **17**, 1433 (1997).
3. E. R. Cook, R. D. D'Arrigo, M. E. Mann, *J. Clim.* **15**, 1754 (2002).
4. H. H. Lamb, *Palaeogeogr. Palaeoclimatol. Palaeoecol.* **1**, 13 (1965).
5. J. Esper, E. R. Cook, F. H. Schweingruber, *Science* **295**, 2250 (2002).
6. J. Esper *et al.*, *Geophys. Res. Lett.* **34**, L17702 (2007).
7. C. J. Proctor, A. Baker, W. L. Barnes, R. A. Gilmour, *Clim. Dyn.* **16**, 815 (2000).
8. The NAO is defined by an atmospheric seesaw between the Icelandic Low and the Azores High and is expressed as an index as the normalized December-to-March sea-level pressure difference between these two poles (*12*).
9. Materials and methods are available as supporting material on *Science* Online.
10. T. D. Mitchell, T. R. Carter, P. D. Jones, M. Hulme, M. New, *A Comprehensive Set of High-Resolution Grids of Monthly Climate for Europe and the Globe: The Observed Record (1901-2000) and 16 Scenarios (2001-2100)* (Working Paper 55, Tyne Centre for Climate Change Research, Univ. of East Anglia, Norwich, UK, 2004).
11. J. W. Hurrell, *Science* **269**, 676 (1995).
12. D. Frank, U. Büntgen, R. Böhm, M. Maugeri, J. Esper, *Quat. Sci. Rev.* **26**, 3298 (2007).
13. M. F. Glueck, C. W. Stockton, *Int. J. Climatol.* **21**, 1453 (2001).
14. J. Luterbacher, C. Schmutz, D. Gyalistras, E. Xoplaki, H. Wanner, *Geophys. Res. Lett.* **26**, 2745 (1999).
15. A. Mangini, C. Spotl, P. Verdes, *Earth Planet. Sci. Lett.* **235**, 741 (2005).
16. J. Luterbacher *et al.*, *Clim. Dyn.* **18**, 545 (2002).
17. A. Pauling, J. Luterbacher, C. Casty, H. Wanner, *Clim. Dyn.* **26**, 387 (2006).
18. N. E. Graham *et al.*, *Clim. Change* **83**, 241 (2007).
19. E. Roeckner, L. Bengtsson, J. Feichter, J. Lelieveld, H. Rodhe, *J. Clim.* **12**, 3004 (1999).
20. C. M. Ammann, F. Joos, D. S. Schimel, B. L. Otto-Bliesner, R. A. Tomas, *Proc. Natl. Acad. Sci. U.S.A.* **104**, 3713 (2007).
21. M. E. Mann, M. A. Cane, S. E. Zebiak, A. Clement, *J. Clim.* **18**, 447 (2005).
22. J. Emile-Geay, M. Cane, R. Seager, A. Kaplan, P. Almasi, *Paleoceanography* **22**, PA3210 (2007).
23. J. W. Hurrell, M. P. Hoerling, A. Phillips, T. Y. Xu, *Clim. Dyn.* **23**, 371 (2004).
24. M. P. Hoerling, J. W. Hurrell, T. Y. Xu, *Science* **292**, 90 (2001).
25. L. Stott *et al.*, *Nature* **431**, 56 (2004).
26. K. M. Cobb, C. D. Charles, H. Cheng, R. L. Edwards, *Nature* **424**, 271 (2003).
27. T. L. Delworth, R. J. Greatbatch, *J. Clim.* **13**, 1481 (2000).
28. A. Timmermann *et al.*, *J. Clim.* **20**, 4899 (2007).
29. W. C. Palmer, *Meteorological Drought* (Research paper 45, U.S. Department of Commerce, Washington, DC, 1965).
30. T. J. Crowley, *Science* **289**, 270 (2000).

31. J.E., D.C.F., and J.D.S. were supported by the European Commission MILLENNIUM Integrated Project (grant 017008) and J.E. and D.C.F. by the Swiss National Science Foundation through the National Centre for Competence in Climate Research (NCCR-Climate). N.E.G. is grateful for support from National Oceanic and Atmospheric Administration (grant NA06OA-R4310120), and J.D.S. acknowledges a Royal Society–Leverhulme Trust Senior Research Fellowship. We thank C. Ammann, E. R. Cook, D. Lund, J. Luterbacher, M.-A. Sicre, J. Smith, D. Stephenson, and three anonymous referees for supplying data and useful suggestions.

Supporting Online Material

www.sciencemag.org/cgi/content/full/324/5923/78/DC1
Materials and Methods
SOM Text
Figs. S1 to S5
Tables S1 and S2
References

24 September 2008; accepted 19 February 2009
10.1126/science.1166349